

Small-angle X-ray scattering and rheological studies on the ordering process of cylindrical microdomains in a polystyrene-*block*-polyisoprene copolymer

Takeji Hashimoto^{a,*}, Toshihiro Ogawa^{†,a}, Naoki Sakamoto^a, Makoto Ichimiya^a, Jin Kon Kim^b and Chang Dae Han^c

^aDepartment of Polymer Chemistry, Graduate School of Engineering, Kyoto University, Kyoto 606-01, Japan

^bDepartment of Chemical Engineering, Pohang University of Science and Technology, Pohang, Kyungbuk 790-784, Korea

^cDepartment of Polymer Engineering, The University of Akron, Akron, OH 44325, USA
 (Received 17 January 1997; revised 30 April 1997)

Ordering of cylindrical microdomains in a low molecular weight polystyrene-*block*-polyisoprene (SI diblock) copolymer was investigated using small-angle X-ray scattering (SAXS) and rheology. The SI diblock copolymer was found to have (i) hexagonally packed cylindrical microdomains of polystyrene phase in a polyisoprene matrix in the ordered state, and (ii) an order–disorder transition temperature T_{ODT} of ca. 90°C. To investigate the ordering process from the disordered state, a specimen was quenched rapidly from the disordered state to a temperature below its T_{ODT} , and then the time evolution of the SAXS intensity and dynamic moduli (G' and G'') (i.e. the ordering process) was monitored. We have found that the ordering process in the block copolymer, when quenched to an ordered state close to its T_{ODT} , takes place very slowly. Specifically, we found that when a specimen was quenched rapidly from 100°C (10°C above T_{ODT}) to 80°C (10°C below T_{ODT}), the ordering into the hexagonally packed cylinders occurs via a nucleation-growth process and the attainment of the equilibrium microdomain morphology took about 6 h when monitoring G' and G'' and about 8 h when monitoring the SAXS intensity. © 1997 Elsevier Science Ltd. All rights reserved.

(Keywords: block copolymers; ordering process; SAXS)

INTRODUCTION

During the past two decades, numerous studies have been reported on order–disorder transitions (ODT) in block copolymers. There are too many papers to cite them all here and the readers are referred to two most recent papers^{1,2} and references therein. However, only during the past few years have studies on the ordering process in block copolymers, when cooled from the disordered state, appeared in the literature^{3–11}. In the investigation of the ordering process in block copolymer, the majority of the studies reported so far made use of time-resolved small-angle X-ray scattering (SAXS) and/or dynamic viscoelastic measurements.

According to the Leibler theory¹² which is based on random phase approximation, when a block copolymer is cooled from the disordered state crossing its order–disorder transition temperature T_{ODT} , it may first form spherical microdomains, then hexagonally packed cylindrical microdomains and finally lamellar microdomains. To date, however, no experimental study has been reported confirming such a prediction, although experimental observations^{13–17} have been reported on a morphology transition between hexagonally packed cylinders and spheres or

between lamellae and hexagonally packed cylinders by annealing at a constant temperature or varying temperature, confirming the Leibler theory. A better understanding of the ordering process in block copolymers is of fundamental importance in controlling microdomain structure, especially in obtaining equilibrium morphology.

In this paper we report the results of our recent experimental study on the ordering process of cylindrical microdomains in a polystyrene-*block*-polyisoprene copolymer when rapid quenching was applied to a specimen from the disordered state. For the study we monitored the time evolution of the SAXS intensity and dynamic moduli using a cone-and-plate rheometer.

EXPERIMENTAL DETAILS

Material

A low molecular weight polystyrene-*block*-polyisoprene (SI diblock) copolymer, having (i) number-average molecular weights M_n of 6000 for PS block and 11700 for PI block as determined by membrane osmometry and (ii) polydispersity index M_w/M_n of 1.09 as determined by gel permeation chromatography, was synthesized via anionic polymerization in our laboratory. Previously we reported that this block copolymer (designated SI-Z) has (i) a T_{ODT} of 90°C as determined by rheology¹ and (ii) hexagonally

* Corresponding author

† Present address: Research Laboratory, Japan Synthetic Rubber Co. Ltd., Yokaichi City, Mie 510, Japan

packed cylindrical microdomains of polystyrene (PS) in a polyisoprene (PI) matrix as determined by transmission electron microscopy (TEM)¹ and SAXS² respectively.

Sample preparation

Samples were prepared by first dissolving a predetermined amount of SI-Z (10 wt.%) in toluene in the presence of an antioxidant (Irganox 1010, Ciba-Geigy Group) and then slowly evaporating the solvent. The evaporation of solvent was carried out slowly at room temperature for 1 week in a fume hood and then in a vacuum oven at 40°C for 3 days. The last trace of solvent was removed by drying the samples in a vacuum oven at an elevated temperature by gradually raising the oven temperature from 40°C to about 10°C above the glass transition temperature of the PS phase ($T_{g,PS}$) in SI-Z. The drying of the samples was continued until there was no further change in weight. Finally, the samples were annealed for 10 h at 83°C, which is 20°C above the $T_{g,PS}$ of SI-Z.

SAXS experiments

SAXS experiments were conducted under a nitrogen atmosphere during the heating and cooling cycles, using an apparatus described in detail elsewhere^{18,19}, which consists of a newly replaced 18 kW rotating-anode X-ray generator operated at 45 kV \times 400 mA (MAC Science, Japan), a graphite crystal for incident-beam monochromatization, a 1.5 m camera, and a one-dimensional position-sensitive proportional counter. The Cu K α line (0.154 nm) was used. The SAXS profiles were measured as a function of temperature and were corrected for absorption, air scattering, and background scattering arising from thermal diffuse scattering, and slit-height and slit-width smearing²⁰. The absolute SAXS intensity was obtained using the nickel-foil method²¹. In the present study, the temperature dependence of SAXS profiles was obtained with a large temperature increment (referred to hereafter as *low temperature-resolution* SAXS experiment) and also with a small temperature increment (referred to hereafter as *high temperature-resolution* SAXS experiment) in a temperature enclosure which was sealed by nitrogen gas. This new temperature enclosure and temperature controller enabled us to control the sample temperature to within $\pm 0.002^\circ\text{C}$.

Rheological measurements

A Rheometrics Dynamic Spectrometer (RDS-2) was used in the oscillatory mode with cone-and-plate fixture (25 mm diameter). Dynamic frequency sweep experiments were conducted, i.e. (1) dynamic storage and loss moduli (G' and G'') were measured as functions of angular frequency ω ranging from 0.01 to 100 rad s^{-1} at various temperatures, during the cooling cycle, from 110 to 75°C in order to determine T_{ODT} of an as-cast SI-Z specimen after being annealed at 83°C (20°C above the T_g) for 10 h, and (2) G' and G'' were measured as functions of ω ranging from 0.05 to 100 rad s^{-1} at 80°C in the ordered state after a specimen was quenched rapidly from 100°C in the disordered state. Also, the time evolution of G' and G'' was monitored at $\omega = 0.05 \text{ rad s}^{-1}$ after a specimen was quenched rapidly from 100°C in the disordered state to 70 or 80°C in the ordered state. The temperature control was accurate to within $\pm 1^\circ\text{C}$ and a fixed strain γ_0 of 0.15 was used at a given temperature, to ensure that measurements were taken well within the linear viscoelastic range of the polymer investigated. All the rheological measurements were conducted under a nitrogen atmosphere in order to avoid oxidative degradation of the samples.

RESULTS AND DISCUSSION

Temperature dependence of SAXS profiles

The temperature dependence of SAXS profiles of the block copolymer is shown in *Figure 1* during the heating and cooling cycles respectively. The thermal program employed in the SAXS experiments is given in *Figure 2*. In *Figure 1* we observe an abrupt change in SAXS profile at temperatures between 87 and 91°C during the heating cycle, but it is less obvious during the cooling cycle. Note that the profiles at 89°C lie between those at 87 and 91°C, which is more clearly indicated in *Figure 3*.

Figure 3 gives plots of (a) the reciprocal of the maximum scattered intensity ($1/I_m$) versus the reciprocal of absolute temperature ($1/T$), (b) the square of half-width at half-maximum (σ_q^2) of the first-order scattering maximum versus $1/T$, and (c) wavelength ($D = 2/\pi/q_m$) of a dominant mode (q_m) of concentration fluctuations versus $1/T$, which

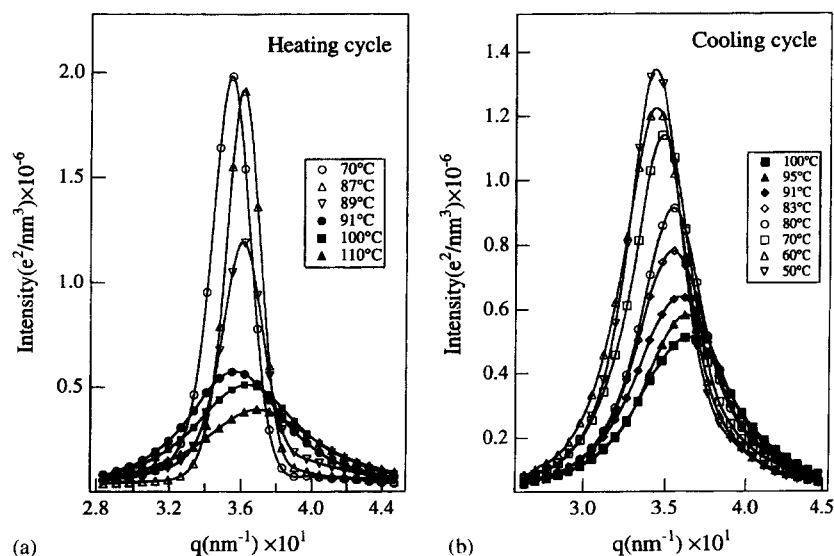


Figure 1 Temperature dependence of the scattering profiles during (a) heating and (b) cooling cycles of SI-Z.

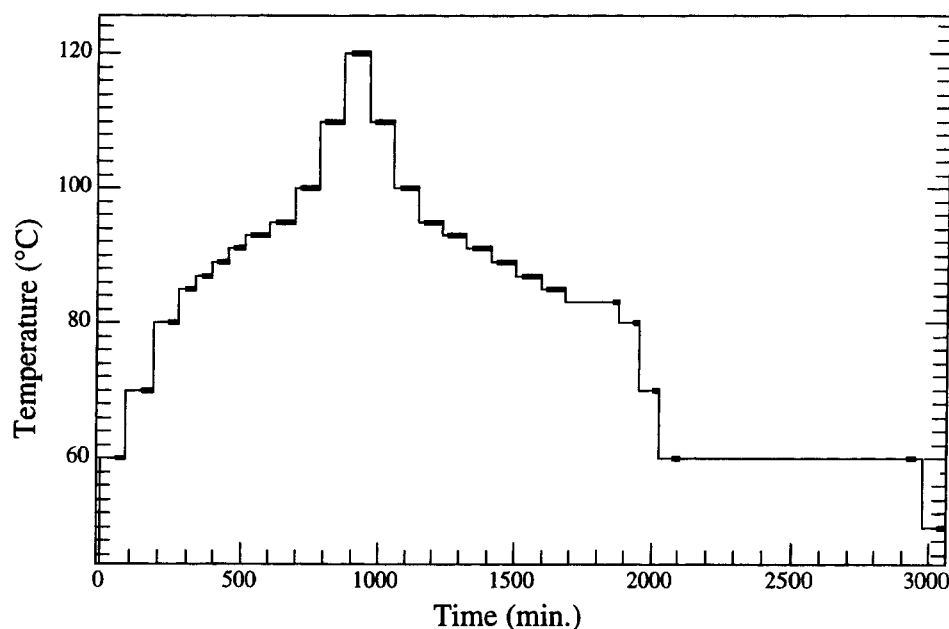


Figure 2 Temperature protocol employed in the SAXS experiment. At each temperature the specimen was held for a specified time (shown by thin horizontal line) and then SAXS measurement was performed for another specified time (shown by thick horizontal line)

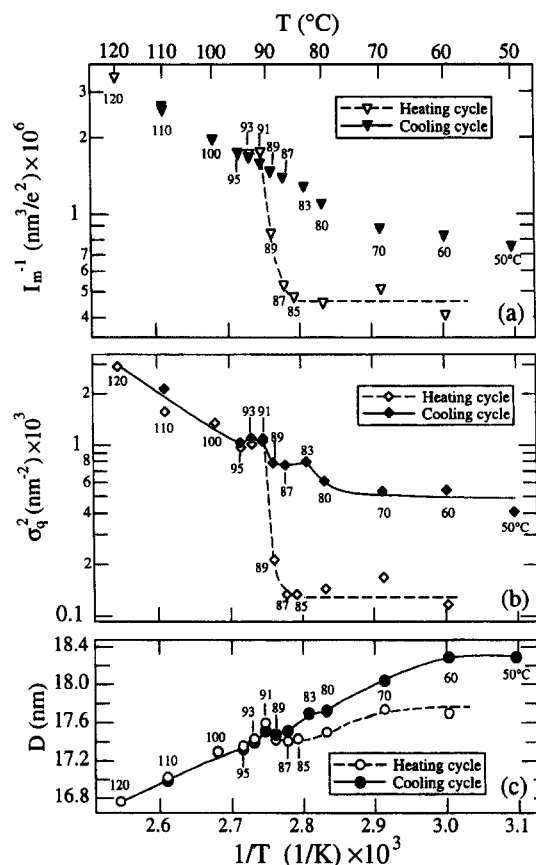


Figure 3 Plots of (a) I_m^{-1} versus $1/T$, (b) σ_q^2 versus $1/T$, and (c) D versus $1/T$ for SI-Z during the heating (broken lines) and cooling cycles (solid lines)

were obtained during the heating and cooling cycles, respectively, for SI-Z. The following observations are worth noting in the SAXS results presented in Figure 3. Both $1/I_m$ and σ_q^2 increase sharply with increasing temperature; specifically, they start to increase sharply at $T \geq 87^\circ\text{C}$ and level off at $T \approx 91^\circ\text{C}$, leading us to conclude that SI-Z is in an ordered state at $T \leq 87^\circ\text{C}$ and in the

disordered state at $T \geq 91^\circ\text{C}$. Thus, the ordered and disordered states coexist at $87^\circ\text{C} < T < 91^\circ\text{C}$. These behaviors are consistent with our previous results except for a difference in the temperature at which $1/I_m$ and σ_q^2 undergo the sharp changes^{22,23}. If we define T_{ODT} as a temperature at which an ordered state disappears completely, then we have $89^\circ\text{C} < T_{\text{ODT}} < 91^\circ\text{C}$, and therefore we assign 90°C to be the T_{ODT} of SI-Z. This value is in excellent agreement with that determined by rheology in our previous study¹. Notice further that D also shows a discontinuous change over the temperature range, $89^\circ\text{C} < T < 91^\circ\text{C}$, where the ordered and disordered phases coexist.

In reference to the SAXS results obtained during the cooling cycle presented in Figure 3, we make the following observations. (1) At $T \geq 93^\circ\text{C}$, the SAXS results obtained during the cooling and heating cycles overlap (i.e. there is no hysteresis effect at $T \geq 93^\circ\text{C}$). However, at $T < 93^\circ\text{C}$, the values of $1/I_m$, σ_q^2 , and D obtained during the cooling cycle are greater than those obtained during the heating cycle. (2) Although the values of $1/I_m$ and σ_q^2 obtained during the cooling cycle show a small discontinuous change at $87^\circ\text{C} < T < 91^\circ\text{C}$, they do not change much, compared with the change during the heating cycle at $87^\circ\text{C} < T < 91^\circ\text{C}$. (3) The values of $1/I_m$ and σ_q^2 obtained during the cooling cycle change significantly at $80^\circ\text{C} < T < 83^\circ\text{C}$, which is believed to be associated with ordering into cylindrical microdomains.

In order to confirm that SI-Z indeed has hexagonally packed cylindrical microdomains in an ordered state, we took two-dimensional (2D) SAXS patterns for a shear-oriented sample with a 2D-SAXS instrument, which was attached with an imaging plate as a 2D detector²⁴. The shear alignment was achieved by applying a large-amplitude oscillatory strain with a strain amplitude of 0.5 and an angular frequency of $4.4 \times 10^{-2} \text{ rad s}^{-1}$ for 2 h at 70°C . The shear-oriented cylinders were stable with annealing at temperatures in an ordered state and at room temperature as well. 2D-SAXS patterns obtained from the two directions are shown in Figure 4. The end pattern in part (a), which was taken with incident X-ray beam parallel to the shear displacement vector (x -axis), shows the hexagonal

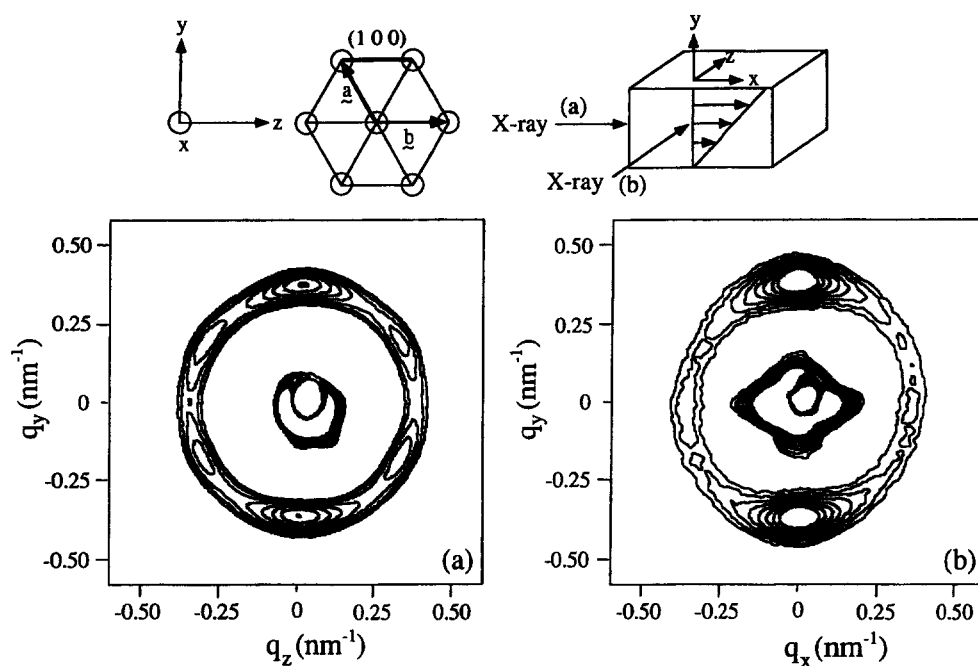


Figure 4 2D SAXS patterns for a shear-oriented sample of SI-Z at 70°C, where the specimen was subjected to large amplitude oscillatory shear for 2 h with an amplitude of 0.5 and an angular frequency of $4.4 \times 10^{-2} \text{ rad s}^{-1}$

diffraction spots, and the edge pattern in part (b), which was taken with the incident beam parallel to the neutral axis (z -axis), shows two-point SAXS pattern oriented parallel to the velocity gradient direction (y -axis). These patterns clearly confirm that SI-Z has a hexagonally packed cylindrical phase in an ordered state. In this particular case, the cylinders are oriented with their axes parallel to the x -axis and (100) plane parallel to the xz -plane (film surface).

Time evolution of microdomain structure as observed by SAXS

Figure 5 describes the time evolution of SAXS profiles near the first-order scattering maximum after a rapid quench from 95°C in the disordered state to 80°C in an ordered state. In obtaining the results given in Figure 5, a sample cell was transferred from a heated metal block controlled at 95°C to another heated metal block controlled at 80°C and placed in the SAXS optical path. We found that temperature equilibration took less than 2 min. The following observations are worth noting in Figure 5. (1) After the quench from 95 to 80°C, the scattering intensity increases and the scattering vector q_m at the maximum scattering intensity shifts to a larger value (i.e. q_m shifts from 0.354 nm^{-1} at 95°C to 0.361 nm^{-1} at 80°C). More precisely, (2) the scattering profile becomes first close to that at 91°C, the disordered state very near the T_{ODT} of SI-Z (see Figure 1) as seen in profiles 1 and 2. (3) The SAXS profile does not change with time up to ca. 2 h (i.e. the SAXS profile remains at 91°C although the system has already been equilibrated at 80°C). (4) Then the SAXS profile changes slowly with time, the maximum intensity I_m increasing and q_m shifting to a larger value and eventually reaching a constant profile after ca. 8 h.

On the basis of the observations made above, we speculate that, upon quenching, the concentration fluctuations in the disordered state at 95°C will relax quite fast to those at 91°C, much faster than the observed time scale of 1 h. The disordered state attained at 80°C is very close to that at 91°C. The ordering process selects particular Fourier modes to grow, as is evident from the fact that the intensity

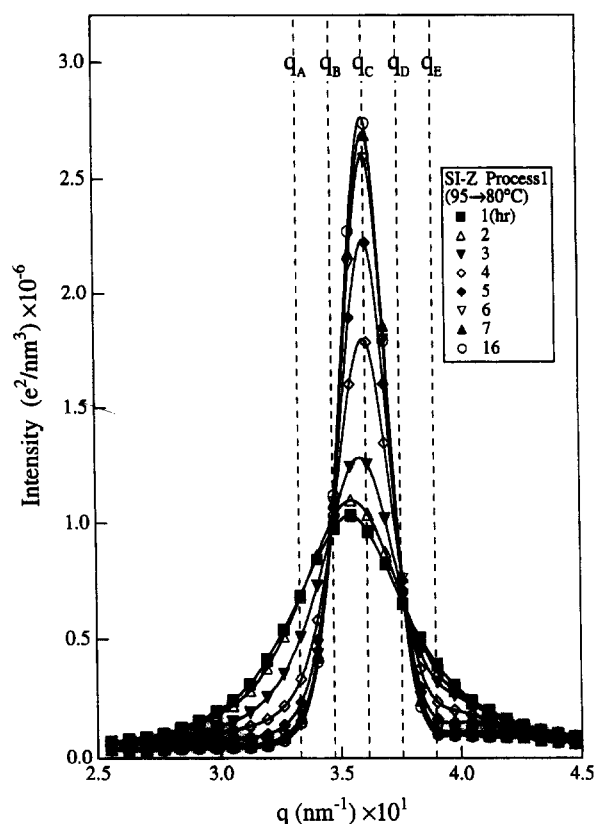


Figure 5 Time evolution of SAXS profiles of SI-Z near the first-order scattering maximum after a rapid quench from the disordered state at 95°C to an ordered state at 80°C

at $q_B < q < q_D$ increases with time but the intensity at $q < q_B$ or $q > q_D$ decreases with time. This is further elaborated on in Figure 6. Figure 6(a) describes the time evolution of the scattered intensity at scattering vectors q_A to q_E (see Figure 5). Specifically, particular Fourier modes ($q_B < q < q_D$, e.g. q_C) grow at the expense of other Fourier modes ($q < q_B$, $q > q_D$, e.g. q_A and q_E). This result reveals the following

points: (i) a non-linear ordering process takes place where mode-mode couplings are involved; (ii) thus the process cannot be described by the Cahn-Hilliard-Cook type theories developed for spinodal decomposition of block copolymer^{25,26}. Figure 6(b) describes the time evolution of σ_q , and Figure 6(c) describes the time evolution of q_m ,

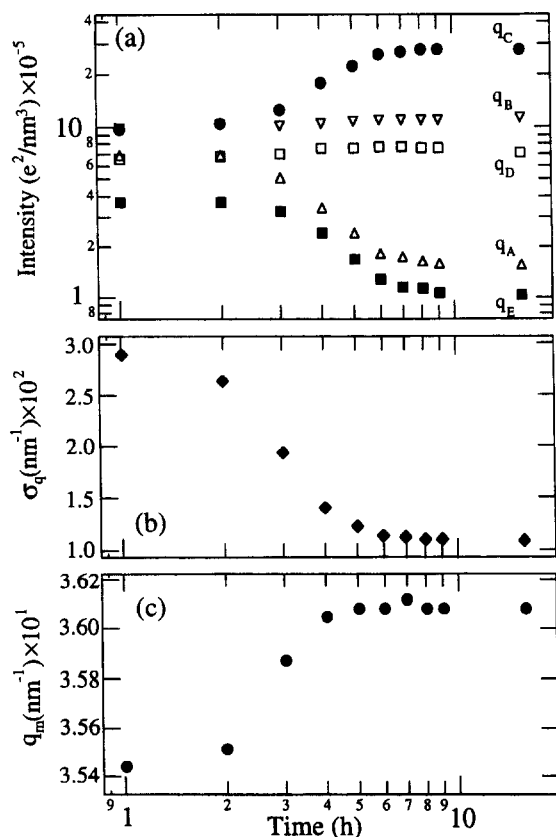


Figure 6 Time evolution of (a) SAXS intensity at particular scattering vectors q_A to q_E shown in Figure 5, (b) σ_q , and (c) q_m for SI-Z

during the ordering process, in which we observe that σ_q decreases while q_m increases with time. Both trends indicate an increasing order with time. The results presented in Figure 6 reveal that the ordering starts after an incubation time, suggesting an ordering via nucleation and growth^{4,9,27,28}.

Figure 7 gives a thermal program employed to obtain the experimental results shown in Figure 8. Figure 8 describes the time evolution of I_m (open circles) and q_m^{-1} (triangles) for SI-Z (i) in process 1 during which a specimen was cooled down from 95 to 80°C and annealed there for 17 h, (ii) in process 2 during which the specimen was heated from 80 to 87°C and then annealed there for 8 h, (iii) in process 3 during which the specimen was heated from 87 to 90°C and then annealed there for 37 h, and (iv) in process 4 during which the specimen was cooled down from 90 to 87°C and annealed there for 28 h. Note that the time evolution of I_m and q_m in processes 1 and 2 are well expected from the static data in Figure 3. The following observations are worth noting in Figure 8. (1) Process 1 describes a disorder-order transition which involves an increase of both I_m and q_m . (2) Process 2 describes the ordering at 80°C and 87°C toward ODT, thus I_m decreases with time. Note, however, that q_m does not change with time.

In reference to Figure 8, the time evolutions of I_m and q_m in processes 3 and 4 are intriguing; namely, process 3 describes the disordering from an ordered state very near ODT (i.e. a state where the disordering tends to start) to a state where the disordering is just completed (see Figure 3), and process 4 describes the process just opposite to that of process 3. In process 3, the scattering intensity first decays to an intermediate level in between the intensity at 87°C (the ordered state near the onset of ODT) and that at 90°C (ordered state near the completion of ODT) and eventually to that at 90°C in the time scale of the order of 1 h. The intermediate scattering intensity level is maintained for about 6 h, although the level tends to decrease slightly with time. The scattering intensity level further decays to that in the disordered state at 90°C within the next 1 h, i.e. from 7 to

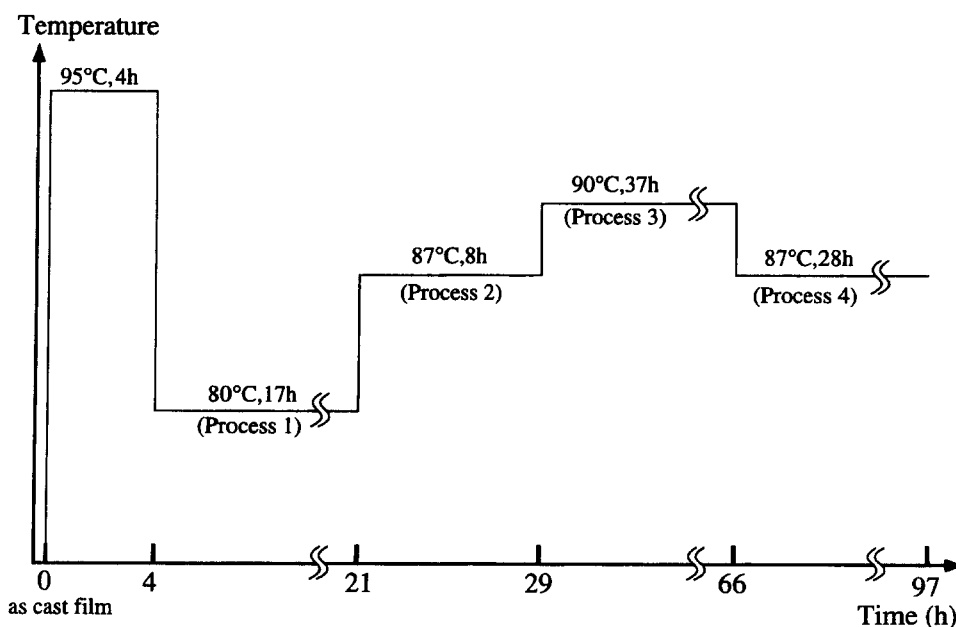


Figure 7 Temperature protocol employed in the ordering and disordering processes of SI-Z: (i) process 1 during which a specimen was cooled from 95 to 80°C and then annealed there for 17 h; (ii) process 2 during which the specimen was heated from 80 to 87°C and then annealed there for 8 h; (iii) process 3 during which the specimen was heated from 87 to 90°C and then annealed there for 37 h; (iv) process 4 during which the specimen was cooled from 90 to 87°C and annealed there for 28 h

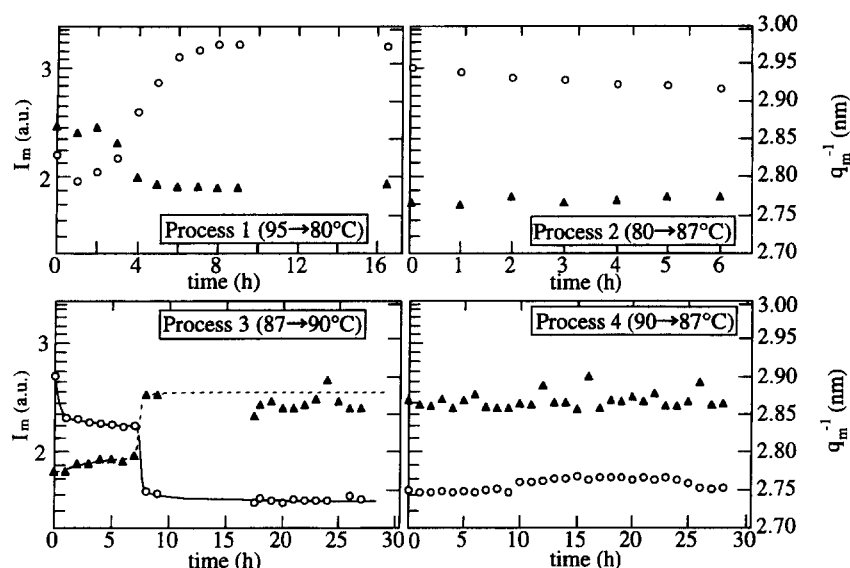


Figure 8 Time evolution of I_m (○) and q_m^{-1} (▲) for SI-Z in processes 1–4, the thermal histories of which are given in Figure 7

8 h after the temperature change. Corresponding to the time change in I_m , q_m decreases slightly and hence D increases slightly up to 7 h. Then it suddenly decreases from 7 to 8 h after the temperature change. Thus, the ODT very near T_{ODT} and the two-phase coexistence region involves a two-step disordering process. Detailed analyses and interpretation of this intriguing phenomenon deserve future investigation. In process 4, both I_m and q_m show that the system remains disordered for such a long time scale as that covered in this experiment, revealing that the disorder–order transition very close to the ODT and nearly in the two-phase coexistence region may involve an extremely long incubation time. It is also intriguing to note that the scattering intensity shows remarkable fluctuations with time during the incubation time. The two-step disordering process and the extremely long incubation time should be further investigated in the future. In order to understand these puzzling results, it may be useful to observe 2D-SAXS patterns as a function of time.

Time evolution of dynamic linear viscoelastic properties with annealing at $T < T_{ODT}$

In order to investigate the effect of thermal history on the rheological behavior of SI-Z in an ordered state, two types of experiments were performed. (1) An as-cast specimen was further annealed in a vacuum oven at 80°C for 1 or 2 weeks and then subjected to small-amplitude ($\gamma_0 = 0.15$) oscillatory shear deformation at various angular frequencies. All the measurements were carried out at 80°C. (2) An as-cast specimen was first heated to the disordered state (100°C) and then quenched rapidly to a preset temperature (70 or 80°C) in an ordered state and the dynamic moduli were monitored using small-amplitude ($\gamma_0 = 0.15$) oscillatory shear deformation at $\omega = 0.05 \text{ rad s}^{-1}$. It should be remembered that the T_{ODT} of the block copolymer is 90°C.

Figure 9 gives plots of (a) $\log G'$ versus $\log \omega$ and (b) $\log G'$ versus $\log G''$ for (1) an as-cast specimen without annealing (open circles), (2) an as-cast specimen after being annealed at 80°C for 1 week (open triangles), and (3) an as-cast specimen after being annealed at 80°C for 2 weeks (open squares). In Figure 9(a) (upper panel) we observe that the slope of the $\log G'$ versus $\log \omega$ plot in the low frequency range ($\omega < 0.1 \text{ rad s}^{-1}$) is much smaller in the annealed specimens than in the unannealed specimen, but $\log G'$

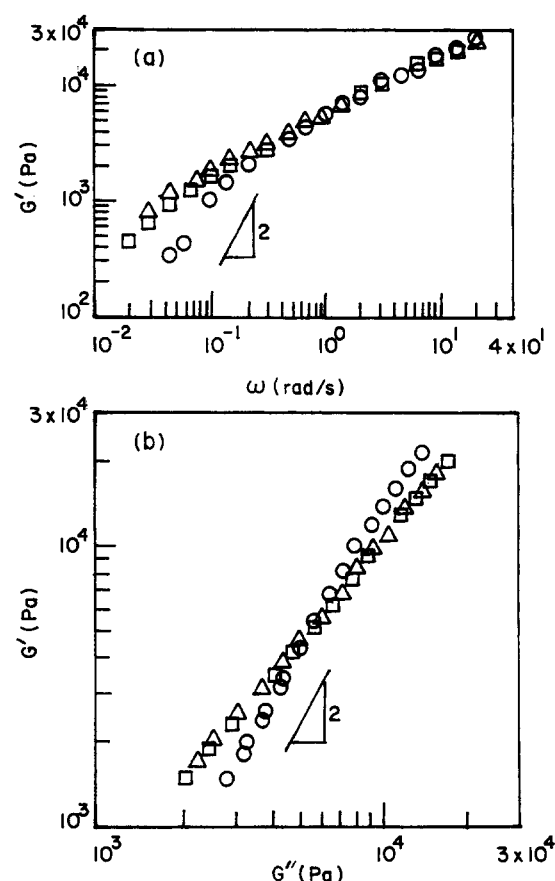


Figure 9 Plots of (a) $\log G'$ versus $\log \omega$ and (b) $\log G'$ versus $\log G''$ for SI-Z having different thermal histories: (○) as-cast specimen without thermal treatment; (△) as-cast specimen after being annealed at 80°C for 1 week; (□) as-cast specimen after being annealed at 80°C for 2 weeks. All measurements were carried out at 80°C

versus $\log \omega$ plots do not reveal much about the effect of annealing on the morphological state of the as-cast specimens. However, Figure 9(b) (lower panel) shows a distinct difference in the rheological response between the annealed and unannealed as-cast specimens, i.e. plots of $\log G'$ versus $\log G''$ for annealed specimens have a slope much less than that for unannealed specimens, indicating that the morphology of the specimen changed during annealing. There is

ample experimental evidence that $\log G'$ versus $\log G''$ plots are very sensitive to the morphological state of block copolymers and the slope of $\log G'$ versus $\log G''$ plots becomes smaller as the morphology of a block copolymer moves farther away from the disordered state²⁹⁻³¹. Thus we can infer from Figure 9(b) that annealing of an as-cast specimen at 80°C for 1 or 2 weeks helped its microdomain structure to change toward an equilibrium morphology.

It is now well understood that the ordered block copolymers have a couple of stress generating mechanisms: (i) orientation and deformation of individual block chains and (ii) deformation of microdomains and grains composed of microdomains. Qualitatively we may assess that the moduli at $\omega > 0.1 \text{ rad s}^{-1}$ correspond to mechanism (i) and those at $\omega < 0.1 \text{ rad s}^{-1}$ to mechanism (ii). Our interest is focused on the time evolution of low frequency behavior which is sensitive to the time evolution of microdomains and grains.

It should be mentioned that the slope 2 in the plot of $\log G'$ versus $\log G''$ observed in the low frequency region in Figure 9(b) for as-cast specimen cannot be ascribed to the thermal concentration fluctuations in the disordered state. If this were to reflect the thermal fluctuation effects in the disordered state, the slope of $\log G'$ versus $\log G''$ plots would have been constant and independent of the annealing time. Thus the liquid-like behavior observed for the as-cast specimen is ascribed to defects in an ordered state. As the defects decrease with annealing, the system changes from liquid-like to soft solid-like behavior, exhibiting the slope less than 2 in the $\log G'$ versus $\log G''$ plot. Here, we define (i) the liquid-like state to be a state at which the cylindrical microdomain of SI-Z has not yet attained a higher degree of ordering in a grain and between grains (grains being surrounded in the disordered phase), and (ii) the solid-like state to be a state at which the cylindrical microdomain of SI-Z has already attained a higher degree of ordering in a grain and the grains fill the whole space, the domains are interconnected at grain boundaries. In reference to Figure 9, it should be remembered that as-cast specimens were annealed in a vacuum oven (i.e. under quiescent conditions) for 1–2 weeks. Thus, the change from liquid-like to soft solid-like behavior, observed in this study, of as-cast specimens during annealing under quiescent conditions, must be distinguished from a situation where a decrease in the amount of defects was observed under large-amplitude oscillatory shear flow, inducing shear-orientation³². In other words, in our case the grains are randomly oriented so that the cylinder axes themselves are randomly oriented; thus the moduli are directionally independent. On the other hand in the latter case, the grains and hence cylinder axes are oriented, giving rise to anisotropy in the moduli. Under such circumstances, a decrease in the amount of defects may result in more or less liquid-like behavior when the shear is applied with its displacement vector parallel to the oriented cylinder axis.

Figure 10 describes the time evolution of G' (open symbols) and G'' (filled symbols) at $\omega = 0.05 \text{ rad s}^{-1}$ with the strain of $\gamma_0 = 0.15$ after an as-cast specimen was quenched rapidly from 100°C in the disordered state to 70 or 80°C in the ordered state. The results given in Figure 10 were obtained using the parallel-plate fixture with the gap opening of 0.7 mm. The following observations are worth noting in Figure 10. (1) When a specimen was quenched from 100 to 80°C, G' increased steadily with time, attaining a constant value after about 8 h, while G'' increased very slowly in the first 2 h and then attained a constant value. (2)

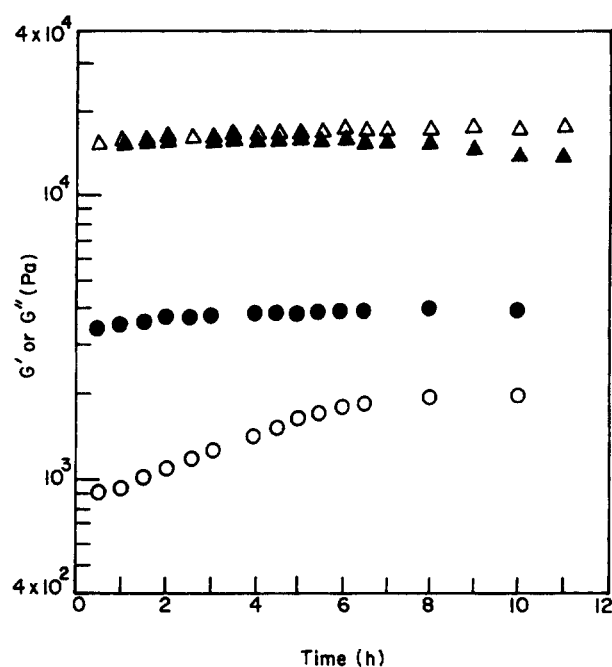


Figure 10 Time evolution of G' and G'' at 0.05 rad s^{-1} for SI-Z specimens: (○) for G' and (●) for G'' after being quenched from 100 to 80°C, and (△) for G' and (▲) for G'' after being quenched from 100 to 70°C

When a specimen was quenched from 100 to 70°C, G' initially increased slightly and then remained more or less constant for the entire period of 11 h, while G'' remained constant for about 6 h and then started to decrease very slowly with time. (3) At 80°C, the equilibrium value of G' is about one half of the equilibrium value of G'' , whereas at 70°C, the equilibrium value of G' is slightly greater than that of G'' . (4) The equilibrium values of G' and G'' at 70°C are much greater than those at 80°C, as may be expected intuitively, because the modulus of PS microdomains in SI-Z would increase as the temperature decreases. The above observations indicate further that the microdomain morphology of a block copolymer would change less with time over the time scale of our observation as the quench depth ΔT is increased from its T_{ODT} . This can be understood from the point of view that the ordering occurs rapidly at the large quench depth (i.e. at 70°C), giving rise to appreciable changes in G' and G'' in the time scale less than 1 h. However, at a smaller quench depth (i.e. at 80°C), the ordering occurs slowly, so that the appreciable changes in G' and G'' occur in the time scale less than 7 h. The time evolution of G' and G'' accompanied by the slow ordering process of the hexagonally packed cylinders was also reported by Winter *et al.*³.

The trend, observed in Figure 10, of the variations of G' and G'' with annealing is at variance with the trend reported in a previous study of Gupta *et al.*³², which shows a decreasing trend of G' and G'' with increasing annealing. These two studies must be distinguished in the following respect. In the present study, small-amplitude ($\gamma_0 = 0.15$) oscillatory shear flow at $\omega = 0.05 \text{ rad s}^{-1}$ was applied, whereas in the study of Gupta *et al.*³², large amplitude ($0.1 \leq \gamma_0 \leq 1.1$) oscillatory shear flow at $\omega = 1 \text{ rad s}^{-1}$ was applied. It has been reported that (1) when large-amplitude oscillatory shear deformation is applied to a microphase-separated block copolymer having lamellar microdomains, which are oriented randomly in a grain, the lamellar microdomains can be aligned along the shearing direction

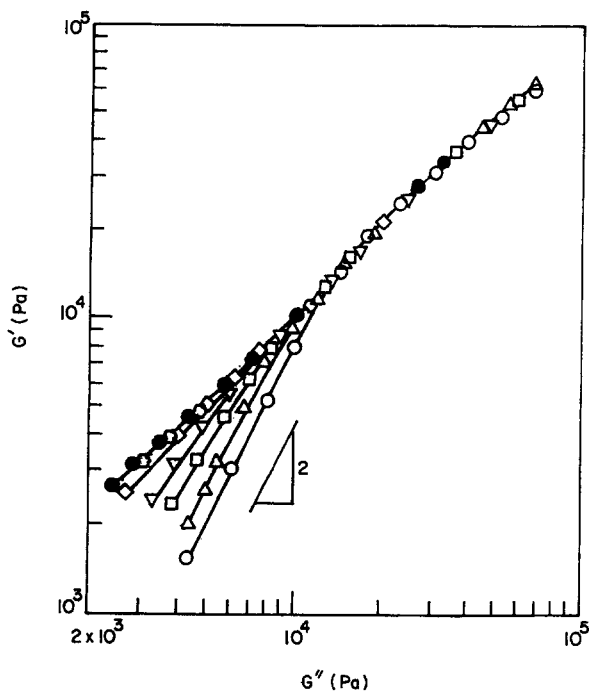


Figure 11 Plots of $\log G'$ versus $\log G''$ for SI-Z specimen, upon being quenched rapidly from 100 to 80°C, at various times: (○) 0.5 h; (△) 2 h; (□) 3 h; (▽) 4 h; (◇) 6 h; (○) 7 h; (●) 8 h

or the gradient of shearing direction, depending upon the values of ω , γ_0 , and temperature employed^{32–34}, and (2) when large-amplitude oscillatory shear deformation is applied to a microphase-separated block copolymer having cylindrical microdomains, which are oriented randomly in a grain, the cylinder axis of the microdomains can be aligned along the shearing direction^{35,36}. Thus, we are led to conclude that the decreasing trend of G' and G'' with increasing annealing reported by Gupta *et al.*³² is attributable to an alignment, which was induced by large-amplitude oscillatory shear flow, of microdomains in a grain.

Figure 11 gives plots of $\log G'$ versus $\log G''$ for SI-Z at 80°C, which were obtained by conducting frequency sweep experiments at every 30 min for the period of 8 h after the specimen had been quenched from 100 to 80°C. It is of interest to observe in Figure 11 that, upon being quenched to 80°C, the slope of the $\log G'$ versus $\log G''$ plot in the terminal region decreased with time until ca. 7 h elapsed and then remained constant. From Figure 11 we can conclude that it takes about 7 h, after the quenching from 100 to 80°C, for the PS microdomains in SI-Z to attain a morphology close to an equilibrium morphology. We shall designate this morphology as an equilibrium morphology hereafter for the sake of convenience.

At this juncture, it is worth elaborating on the physical significance of $\log G'$ versus $\log G''$ plots, given in Figure 11, in the terminal region (say at $G'' \leq 7 \times 10^3$ Pa, which corresponds roughly to $\omega \leq 0.1$ rad s^{-1}), putting emphasis on the ordering process taking place upon quenching. Note that G' describes the energy stored per unit volume and G'' describes the energy dissipated per unit volume when a specimen is subject to an oscillatory shear deformation. In order to facilitate our discussion below, we have prepared Figure 12, where A denotes the rheological (or morphological) state at the very early stage of ordering upon quenching, B and C denote the state at which an equilibrium morphology has not been attained yet, and D denotes the state at which an equilibrium morphology has been attained.

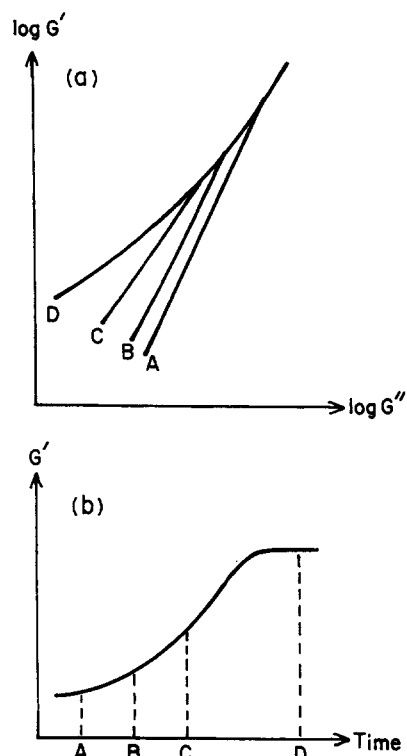


Figure 12 Schematic diagram describing (a) variations of the slope of $\log G'$ versus $\log G''$ plots in the terminal region, and (b) variations of G' with time at a fixed value of ω in the terminal region, upon quenching of SI-Z from the disordered state to an ordered state

Without having information on the morphology of SI-Z at the respective stages (A through D), at present we can only speculate on the morphology corresponding to the storage modulus G' at each stage designated in Figure 12.

At stage A (30 min after the quenching began, in reference to Figure 11) SI-Z has a very low value of G' , implying that the morphology of the block copolymer has changed little from the disordered state, consistent with the time-resolved SAXS results which reveals that the system in this stage is still in the incubation period of time. This speculation is corroborated by the fact that the $\log G'$ versus $\log G''$ plot (see open circles in Figure 11) of SI-Z has the slope of almost 2, signature of the disordered state^{29–31}. At stage B (2 h after the quenching began, in reference to Figure 11), the value of G' has increased somewhat, indicating that microdomains have formed. Note, however, that the $\log G'$ versus $\log G''$ plot (see open triangles in Figure 11) of SI-Z has the slope of almost 2, exhibiting a liquid-like rheological response. This is consistent with only a slight increase of I_m observed in the time-resolved SAXS study.

At stage C (3 h after the quenching began, in reference to Figure 11), the value of G' has increased further, indicating that ordering continued. Note that the $\log G'$ versus $\log G''$ plot (see open squares in Figure 11) of SI-Z still has the slope of almost 2, exhibiting a liquid-like rheological response. We speculate that from the morphological point of view, stages B and C differ from each other in the extent of ordering, and that ordered and disordered states might coexist. It may be conceivable that grains composed of ordered cylinders are dispersed in the disordered matrix and that the volume fraction of this ordered region increases with time in this time domain. As the grain size and its volume fraction increase with time, the position of the line with slope 2 shifts toward the left-hand side, or upward

direction, corresponding to a low-frequency shift of the liquid-like rheological response with time.

At stage D (7–8 h after the quenching began, in reference to *Figure 11*), the value of G' has increased considerably and no longer changes with time, indicating that an equilibrium morphology is attained, consistent with attainment of the constant value of I_m in the time-resolved SAXS study. Note that the $\log G'$ versus $\log G''$ plot (see hexagons and closed circles in *Figure 11*) of SI-Z has the slope of much less than 2, exhibiting a solid-like rheological response. This observation leads us to speculate that grains are volume-filling at stage D and that ordering inside the grains might have attained a state close to equilibrium. It should be emphasized that above we merely presented a number of speculations, consistent with the time evolutions of the SAXS profile and rheological behaviors, in the absence of information on the morphology of SI-Z during ordering, upon quenching from the disordered state to an ordered state. The time evolution of morphology in a block copolymer, upon quenching from the disordered state to an ordered state, is worth investigating in the future.

Finally we add a brief comment on the work done by Balsara *et al.*³⁷. Although they also have considered the effect of grain boundary on linear viscoelasticity, they explored the effects on the low frequency behavior, after the system attained the soft-solid behavior, and concluded that the grain size has little effect on the moduli in the soft-solid region. We think that this conclusion is consistent with our results and speculations. The soft-solid behavior is attained after the system reaches a morphological state in which the grains are volume filling and cylinders in the grains have a spatial order close to equilibrium. In this work we can further propose that the grain size affects significantly the rheological response before the grains fill the whole sample space.

CONCLUDING REMARKS

In this paper, using the experimental results obtained from SAXS and rheological measurements, we discussed the ordering process of cylindrical microdomains in a low molecular weight SI diblock copolymer when it was quenched rapidly from the disordered state to an ordered state. It is very encouraging to observe that both the SAXS and rheological studies show very similar results in that the ordering of cylindrical microdomains, when quenched from 100 to 80°C or from 95 to 80°C, takes about 6–8 h before attaining an equilibrium morphology. We found, however, that when a specimen was quenched to a temperature farther away from its T_{ODT} (i.e. a deep quench), the time evolution of dynamic moduli is very fast, indicating that it will take a very short time to reach an equilibrium morphology. Such information is very useful for the control of microdomain structure in a block copolymer when a specimen was first heated to the disordered state and then cooled down to an ordered state. The SAXS results, particularly *Figure 8* shown in this paper, are very useful for a better understanding of the ordering process (i.e. the kinetics of phase transition) in a block copolymer near its ODT. Further study on this subject is worth pursuing in the future.

REFERENCES

- Han, C. D., Baek, D. M., Kim, J. K., Ogawa, T. and Hashimoto, T., *Macromolecules*, 1995, **28**, 5043.
- Ogawa, T., Sakamoto, N., Hashimoto, T., Han, C. D. and Baek, D. M., *Macromolecules*, 1996, **29**, 2113.
- Winter, H. H., Scott, D. B., Gronski, W., Okamoto, S. and Hashimoto, T., *Macromolecules*, 1993, **26**, 7236.
- Schuler, M. and Stühn, B., *Macromolecules*, 1993, **26**, 112.
- Stühn, B., Vilesov, A. and Zachmann, H. G., *Macromolecules*, 1994, **27**, 3560.
- Floudas, G., Pakula, T., Fischer, E. W., Hadjichristidis, N. and Pispas, S., *Acta Polym.*, 1994, **45**, 176.
- Floudas, G., Hadjichristidis, N., Iatrou, H., Pakula, T. and Fischer, E. W., *Macromolecules*, 1994, **27**, 7735.
- Floudas, G., Fytas, G., Hadjichristidis, N. and Pitsikalis, M., *Macromolecules*, 1995, **28**, 2359.
- Hashimoto, T. and Sakamoto, N., *Macromolecules*, 1995, **28**, 4779.
- Floudas, G., Pispas, S., Hadjichristidis, N., Pakula, T. and Erukhimovich, I., *Macromolecules*, 1996, **29**, 4142.
- Adams, J. L., Quiram, D. J., Graessley, W. W. and Register, R. A., *Macromolecules*, 1996, **29**, 2929.
- Leibler, L., *Macromolecules*, 1980, **13**, 1602.
- Sakurai, S., Momii, T., Taie, K., Shibayama, M., Nomura, S. and Hashimoto, T., *Macromolecules*, 1993, **26**, 458.
- Sakurai, S., Kawada, H., Hashimoto, T., Fetters, L. J. *Proc. Jpn. Acad.*, 1993, **67B**, 13; *Macromolecules*, 1993, **26**, 5796.
- Hajduk, D. A., Gruner, S. M., Rangarajan, P., Register, R. S., Fetters, L. J., Honeker, C., Albalak, R. J. and Thomas, E. L., *Macromolecules*, 1994, **27**, 490.
- Hamley, I. W., Koppi, K. A., Rosedale, J. H., Bates, F. S., Almadal, K. and Mortensen, K., *Macromolecules*, 1993, **26**, 5659.
- Sakamoto, N., Hashimoto, T., Han, C. D., Kim, D. and Vaidya, N. Y., *Macromolecules*, 1997, **30**, 1621.
- Hashimoto, T., Suehiro, S., Shibayama, M., Saijo, K. and Kawai, H., *Polym. J.*, 1981, **13**, 501.
- Suehiro, S., Saijo, K., Ohta, Y., Hashimoto, T. and Kawai, H., *Anal. Chim. Acta*, 1986, **189**, 41.
- Fujimura, M., Hashimoto, T. and Kawai, H., *Mem. Fac. Eng., Kyoto Univ.*, 1981, **43**(2), 224.
- Hendricks, R. W., *J. Appl. Crystallogr.*, 1972, **5**, 315.
- Hashimoto, T., Ogawa, T. and Han, C. D., *J. Phys. Soc. Jpn.*, 1994, **63**, 2206.
- Sakamoto, N. and Hashimoto, T., *Macromolecules*, 1995, **28**, 6825.
- Hashimoto, T., Okamoto, S., Saijo, K., Kimishima, K. and Kume, T., *Acta Polym.*, 1995, **46**, 463.
- Hashimoto, T., *Macromolecules*, 1987, **20**, 465.
- Kawasaki, K. and Sekimoto, K., *Macromolecules*, 1989, **22**, 3063.
- Sakamoto, N. and Hashimoto, T., *Butsuseikenkyu*, 1996, **66**, 488.
- Hashimoto, T., Sakamoto, N. and Koga, T., *Phys. Rev. E*, 1996, **54**, 5832.
- Han, C. D. and Kim, J., *J. Polym. Sci., Polym. Phys. Ed.*, 1987, **25**, 1741.
- Han, C. D., Kim, J. and Kim, J. K., *Macromolecules*, 1989, **22**, 383.
- Han, C. D., Baek, D. M. and Kim, J. K., *Macromolecules*, 1990, **23**, 561.
- Gupta, V. K., Krishnamoorti, R., Kornfield, J. A. and Smith, S. D., *Macromolecules*, 1995, **28**, 4464.
- Riise, B. L., Fredrickson, G. H., Larson, R. G. and Pearson, D. S., *Macromolecules*, 1995, **28**, 7653.
- Koppi, K. A., Tirrel, M., Bates, F. S., Almdal, K. and Colby, R. H., *J. Phys. France, II*, 1992, **2**, 1941.
- Morrison, F. A. and Winter, H. H., *Macromolecules*, 1989, **22**, 3533.
- Morrison, F. A., Winter, H. H., Gronski, W. and Barnes, J. D., *Macromolecules*, 1990, **23**, 4200.
- Balsara, N. P., Dai, H. J., Watanabe, H., Sato, T. and Osaki, K., *Macromolecules*, 1996, **29**, 3507.